Modulation instability in silicon photonic nanowires

Article *in* Optics Letters · January 2007

DOI: 10.1364/OL.31.003609 · Source: PubMed

3 authors, including:

Nicolae C Panoiu
University College London
222 PUBLICATIONS **4,286** CITATIONS
SEE PROFILE

Xiaogang Chen
University of Illinois, Urbana-Champaign
47 PUBLICATIONS **1,029** CITATIONS
SEE PROFILE

Modulation instability in silicon photonic nanowires

Nicolae C. Panoiu, Xiaogang Chen, and Richard M. Osgood, Jr.

Department of Applied Physics and Applied Mathematics, Columbia University, New York, New York 10027

Received July 17, 2006; revised August 28, 2006; accepted September 8, 2006;
posted September 21, 2006 (Doc. ID 73071); published November 22, 2006

We demonstrate that strong modulation instability (MI) of copropagating optical waves can be observed in Si photonic nanowires with a length of only a few millimeters. We consider two distinct cases, namely one in which one wave propagates in the normal group-velocity dispersion (GVD) region and the other one experiences anomalous GVD, and a second case in which both waves propagate in the anomalous GVD region. In both cases we show that, for comparable optical powers, the peak value of the MI gain spectrum is 2 to 3 orders of magnitude larger than that achieved in optical fibers. © 2006 Optical Society of America

OCIS codes: 130.4310, 230.4320, 230.7370, 190.4360.

Silicon photonics has become an important and active current area of photonics research, mainly because the silicon-on-insulator (SOI) platform offers several distinct advantages such as a seamless integration with complementary metal-oxide semiconductor (CMOS) technologies, particularly fabrication, and a high-index-of-refraction contrast, which facilitates optical guiding via very tight modal confinement. These unique properties have already led to several ultrasmall low-loss passive optical devices such as strip waveguides, bends, Y-splitters, and ring resonators.[1–3] In addition, this strong optical field confinement, in connection with the large optical nonlinearity of Si, provides a route for achieving ultradense on-chip nonlinear all-optical photonic integrated circuits. One milestone on this route has recently been reached with the development of optical amplifiers on Si such as Si Raman lasers[4,5] and Raman amplifiers.[6–10] Other nonlinear processes in Si, such as four-wave mixing (FWM)[11–13] or Kerr nonlinearity,[14] can also be employed to achieve active functionality in SOI devices. However, although these schemes can be used to achieve optical gain at specific frequencies, they offer little flexibility for all-optical frequency tuning.

In this Letter we propose an alternative all-optical scheme that can provide optical gain at a tunable frequency. Thus we demonstrate that two optical waves that copropagate in a SOI photonic nanowire present a strong modulation instability (MI), which is manifest within a propagation distance of just a few millimeters. The MI gain depends on the power of the optical waves so that it can be optically tuned, and it will reach its maximum value when both waves experience anomalous group-velocity dispersion (GVD). As a result of the MI, the optical waves develop deep subpicosecond modulations. These findings could play an important role in designing on-chip sources of ultrashort optical pulses. We analyze two cases: case A, in which one wave propagates in the normal GVD region, and the other one experiences anomalous GVD; and case B, in which both waves propagate in the anomalous GVD region.

The SOI nanowire consists of a Si strip with width $w=360$ nm and height $h=220$ nm, placed on top of a thick SiO_2 substrate. The waveguide dimensions are chosen so the SOI nanowire's frequency dispersion is normal (anomalous) for wavelengths $\lambda>\lambda_0=1550$ nm ($\lambda<\lambda_0$). To characterize the dispersion properties of the Si nanowire we determined the optical modes supported by the waveguide, by using BeamPROP, a commercially available software, as well as the frequency dependence of the mode propagation constant, β. These calculations were cross-checked by using a finite-element-based numerical method. Our simulations showed that for $1350\ \text{nm}<\lambda<1850$ nm, the waveguide supports only the TE-like mode E_{11}^x. In addition, we calculated the mode index, n_{eff}, defined by $\beta(\omega)=n_{\text{eff}}\omega/c$; the group index $n_g=c/v_g=\beta_1 c$, where $\beta_1=\mathrm{d}\beta/\mathrm{d}\omega$; and $\beta_2=\mathrm{d}^2\beta/\mathrm{d}\omega^2$, the second-order dispersion coefficient. The results of these computations are illustrated in Fig. 1. This figure shows that n_g has a maximum at λ_0, which means that the waveguide has a zero-dispersion point at $\lambda_0[\beta_2(\lambda_0)=0]$.

The dynamics of two optical waves propagating in an SOI wire is governed by a system of coupled equations[10]

$$i\frac{\partial u_p}{\partial z}+\frac{i}{v_{gp}}\frac{\partial u_p}{\partial t}-\frac{\beta_{2p}}{2}\frac{\partial^2 u_p}{\partial t^2}=-\frac{ic\kappa_p}{2nv_{gp}}(\alpha_{in}+\alpha_{\text{FC}}^p)u_p-\frac{\omega_p\kappa_p}{nv_{gp}}\delta n_{\text{FC}}^p u_p-\frac{3\omega_p}{\varepsilon_0 A_0 v_{gp}}\left(\frac{P_p\Gamma_p}{v_{gp}}|u_p|^2+2\frac{P_s\Gamma_{sp}}{v_{gs}}|u_s|^2\right)u_p,$$

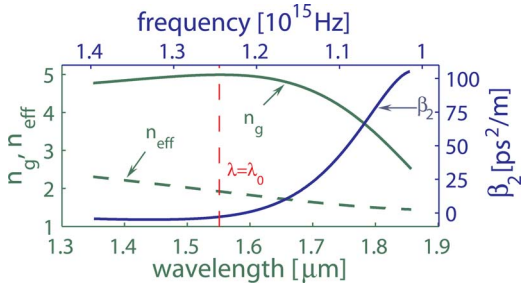

Fig. 1. (Color online) Wavelength and frequency dependence of n_{eff}, n_g, and β_2.

0146-9592/06/243609-3/$15.00

$$i\frac{\partial u_s}{\partial z}+\frac{i}{v_{gs}}\frac{\partial u_s}{\partial t}-\frac{\beta_{2s}}{2}\frac{\partial^2 u_s}{\partial t^2}$$
$$=-\frac{ic\kappa_s}{2nv_{gs}}(\alpha_{in}+\alpha_{\mathrm{FC}}^{s})u_s-\frac{\omega_s\kappa_s}{nv_{gs}}\delta n_{\mathrm{FC}}^{s}u_s$$
$$-\frac{3\omega_s}{\varepsilon_0 A_0 v_{gs}}\left(\frac{P_s\Gamma_s}{v_{gs}}|u_s|^2+2\frac{P_p\Gamma_{ps}}{v_{gp}}|u_p|^2\right)u_s, \quad (1)$$

where $z(t)$ is the distance (time), $u_{p,s}$ are normalized pulse envelopes, $p(s)$ stands for pump (signal), $P_{p,s}$ are the peak powers, $A_0=wh$ is the geometrical area of the Si nanowire, α_{in} is the intrinsic loss, and $\alpha_{\mathrm{FC}}^{p,s}$ ($\delta n_{\mathrm{FC}}^{p,s}$) are the free carrier (FC) losses (FC-induced refractive index change). The parameters $\Gamma_{p,s},\Gamma_{ps,sp}$ are effective waveguide nonlinearities, $\Gamma_j=A_0\int \mathsf{e}_j^*\cdot\hat{\chi}^{(3)}:\mathsf{e}_j\mathsf{e}_j^*\mathsf{e}_j dA/\mathcal{J}_j^2$, $\Gamma_{jl}=A_0\int \mathsf{e}_l^*\cdot\hat{\chi}^{(3)}:\mathsf{e}_j\mathsf{e}_j^*\mathsf{e}_l dA/(\mathcal{J}_j\mathcal{J}_l)$, $(j,l=p,s)$, where $\hat{\chi}^{(3)}$ is the third-order susceptibility of Si, $\mathcal{J}_{p,s}=\int n^2(\mathbf{r}|\mathsf{e}_{p,s}|^2 dA$, and $\mathsf{e}_{p,s}\equiv\mathsf{e}_{p,s}(\omega_{p,s};\mathbf{r})$ are the waveguide modes. To compute these parameters we used[10,15] $\hat{\chi}^{(3)}_{1111}=(5.21+i0.26)\times10^{-19}\,\mathrm{m^2/V^2}$ and $\hat{\chi}^{(3)}_{1122}=(2.5+i0.18)\times10^{-19}\,\mathrm{m^2/V^2}$. Based on a Drude model, δn_{FC} and α_{FC} are given by[16] $\delta n_{\mathrm{FC}}=-(c^2N/2\varepsilon_0 n\omega^2)\times(1/m_{ce}^{*}+1/m_{ch}^{*})$, and $\alpha_{\mathrm{FC}}=(e^3N/\varepsilon_0 cn\omega^2)(1/\mu_e m_{ce}^{*2}+1/\mu_h m_{ch}^{*2})$, where N is the FC density, $m_{ce}^{*}=0.26m_0$ ($m_{ch}^{*}=0.39m_0$) is the effective mass of the electrons (holes), with m_0 the mass of the electron, and μ_e (μ_h) is the electron (hole) mobility. The FC dynamics is determined by a rate equation[10]

$$\frac{\partial N}{\partial t}=-\frac{N}{t_c}+\frac{6}{\varepsilon_0\hbar A_0^2}\left[\frac{P_p^2\Gamma_p''}{2v_{gp}^2}|u_p|^4\frac{P_s^2\Gamma_s''}{2v_{gs}^2}|u_s|^4\right.$$
$$\left.+2\frac{(\omega_p\Gamma_{sp}''+\omega_s\Gamma_{ps}'')P_pP_s}{(\omega_p+\omega_s)v_{gp}v_{gs}}|u_p|^2|u_s|^2\right], \quad (2)$$

where $t_c\sim0.5$ ns is the characteristic lifetime of FCs for our waveguide dimensions, and the double-prime symbol means the imaginary part. Note that in Si nanowires t_c is strongly reduced as compared with bulk Si, because the presence of surface states offers an efficient mechanism for FC recombination.

To investigate the MI of two optical waves whose propagation is described by Eqs. (1) we first determine its steady-state (cw) solutions, i.e., z-independent solutions, and then analyze the linear dynamics of small perturbations of the cw solutions.[17–19] For now we neglect the linear and nonlinear losses; we will discuss their influence on our results later. Thus simple calculations show that the cw solutions of (1), $u_{p,s}^0$, can be written as $u_{p,s}^0=\exp[i(\gamma_{p,s}P_{p,s}+2\gamma_{sp,ps}P_{s,p})z]$, where $\gamma_{p,s}=3\omega_{p,s}\Gamma_{p,s}/(\varepsilon_0A_0v_{gp,s}^2)$, and $\gamma_{ps,sp}=3\omega_{s,p}\Gamma_{ps,sp}/(\varepsilon_0A_0v_{gp}v_{gs})$. If we now consider small plane-wave perturbations of the cw solutions, $u_{p,s}(z,t)=u_{p,s}^0+\delta u_{p,s}(z,t)$, with $\delta u_{p,s}(z,t)=\delta u_{p,s}^0\exp[i(\Lambda z-\Omega t)]$, insert these functions in Eqs. (1), and linearize the corresponding system of equations, we obtain a linear homogeneous system of equations that determines the perturbation amplitudes, $\delta u_{p,s}^0$. The condition for this system to have nontrivial solutions gives the relationship between the wavevector Λ and perturbation frequency Ω:

$$[(\Lambda-\Omega/v_{gp})^2-\varrho_p][(\Lambda-\Omega/v_{gs})^2-\varrho_s]=\eta\Omega^4, \quad (3)$$

where $\varrho_{p,s}=\beta_{2p,s}\Omega^2(\gamma_{p,s}P_{p,s}+\beta_{2p,s}\Omega^2/4)$, and $\eta=4\gamma_{ps}\gamma_{sp}\beta_{2p}\beta_{2s}P_pP_s$. If Eq. (3) has solutions $\Lambda(\Omega)$ so as $\mathrm{Im}[\Lambda(\Omega)]\neq0$ then the perturbation $\delta u_{p,s}(z,t)$ represents an exponentially growing mode. As a result, the MI gain spectrum is given by $G(\Omega)=2\,\mathrm{Im}[\Lambda(\Omega)]$.

Now consider the MI gain in cases A and B. In case A, the pump beam propagates in the normal GVD region, $\lambda_p=1625.3$ nm ($\omega_p=1.16\times10^{15}$ Hz), whereas in case B it experiences anomalous GVD, $\lambda_p=1400$ nm ($\omega_p=1.35\times10^{15}$ Hz). In both cases the signal beam propagates in the anomalous GVD region, at $\lambda_s=1450$ nm ($\omega_s=1.3\times10^{15}$ Hz). In case A we chose the two wavelengths so that the waves have the same group velocity, and thus there is no temporal walk-off, whereas in case B the walk-off parameter is $\delta=|1/v_{gp}-1/v_{gs}|=86.3$ ps/m. By using Eq. (3), we determined the dependence of the gain spectra versus the pump power P_p, for a signal power $P_s=50$ mW in case A, and $P_s=10$ mW in case B. The results, presented in Fig. 2, show that in both cases the copropagating waves experience strong MI, with a bandwidth of the gain spectrum of ~10 THz. Note that although the powers P_p, P_s are smaller in case B, a larger MI gain is observed if both waves experience anomalous GVD. However, note that in both cases the MI gain is $\sim10^2-10^3$ times as large as the MI gain achievable in optical fibers, for similar values of the optical powers. This is because the susceptibility $\hat{\chi}^{(3)}$ of Si is much larger than that of silica, and the modal area of the SOI nanowire is much smaller than that of an optical fiber. As a result, the parameters γ, which determine the strength of the MI gain, are much larger for SOI nanowires as compared with that of optical fibers. Moreover, the coupling losses in Si nanowires are only ~1.5 dB/coupler,[7] so that although they are larger than the coupling losses in optical fibers the large enhancement in the MI gain offsets these increased losses.

The conclusions of our linear-stability analysis are fully verified by direct numerical simulations of Eqs.

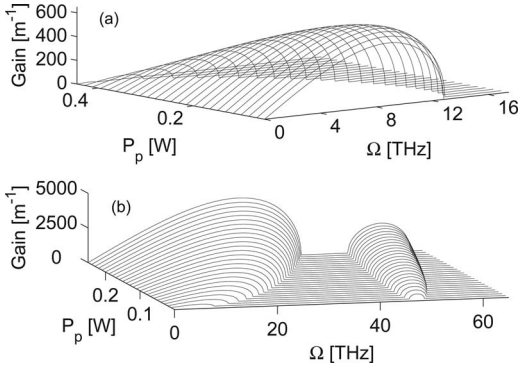

Fig. 2. Calculated MI gain spectra for (a) case A and (b) case B. The powers of the signal wave in cases A and B are $P_s=50$ mW and $P_s=10$ mW, respectively.

(1) and (2). Thus in both cases we launched Gaussian pulses into the waveguide, with the pulse width $T_{0p} = T_{0s} = 10$ ps, and peak powers $P_p = P_s = 250$ mW (case A), and $P_p = P_s = 100$ mW (case B). Our simulations revealed that in both cases the envelopes of the copropagating pulses developed temporal modulation, a manifestation of the onset of the MI [see Figs. 3(b) and 3(d)]. In the pulse spectra, the MI is reflected by the development of exponentially growing sidebands. As Fig. 3 shows, the frequency of the sidebands matches well the frequency at which the MI gain reaches its maximum. Although the pulse dynamics in the two cases shows many similarities, Fig. 3 also illustrates several important differences. First, in case A, the MI sidebands begin to develop only after the central part of the spectrum broadens due to self-modulation and cross-phase modulation, as the generated frequency components act as a seed for the MI. By contrast, in case B, the MI sidebands are well separated from the central part of the spectrum, which means that the MI develops from noise-generated frequencies. Second, unlike in case A, in case B the MI sidebands are asymmetric, an effect that is attributable to the group-velocity mismatch between the pulses. Thus since the MI can be viewed as the result of FWM processes, when the two waves have different group velocity the two FWM processes involving the sidebands have different wave-vector mismatch and thus have different efficiencies. Such asymmetry of the sidebands has been observed in experiments in both optical fibers[18] and SOI waveguides.[13]

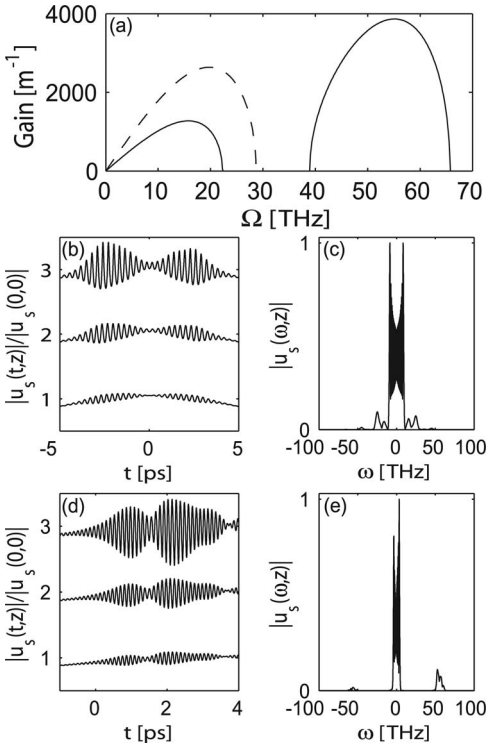

Fig. 3. Results of numerical simulation of MI. (a) Gain spectra for cases A (dashed curve) and B (solid curve); (b) and (c) correspond to case A, (d) and (e) correspond to case B and show the normalized temporal profiles of the signal pulses at $z = 19.5$ mm, $z = 20$ mm, and $z = 20.5$ mm (from bottom to top) and the spectra at $z = 20$ mm, respectively. For clarity, the temporal profiles are shifted by 1. The peak powers are $P_p = P_s = 250$ mW (case A) and $P_p = P_s = 100$ mW (case B).

To summarize, we have demonstrated that strong MI can be observed in Si nanowires with lengths of only a few millimeters. Since the frequency corresponding to the maximum MI gain can be tuned by changing the power of the interacting waves, our results suggest that MI can be employed to design on-chip optical sources with a highly tunable repetition rate. Finally, note that the effective parameters γ of the Si wire are inversely proportional to v_g, which suggests that, similar to the Raman amplification,[20] a much stronger MI could be observed in photonic nanostructures supporting slow-light modes, e.g., photonic crystal waveguides.

This work was supported by U.S. Air Force Office of Scientific Research grants FA9550-04-C-0022 and FA9550-05-1-0428. N. Panoiu's e-mail address is panoiu@cumsl.msl.columbia.edu.

References

1. J. S. Foresi, D. R. Lim, L. Liao, A. M. Agarwal, and L. C. Kimerling, in Proc. SPIE **3007**, 112 (1997).
2. R. U. Ahmad, F. Pizzuto, G. S. Camarda, R. L. Espinola, H. Rao, and R. M. Osgood, IEEE Photon. Technol. Lett. **14**, 65 (2002).
3. Y. A. Vlasov and S. J. McNab, Opt. Express **12**, 1622 (2004).
4. O. Boyraz and B. Jalali, Opt. Express **12**, 5269 (2004).
5. H. Rong, A. Liu, R. Jones, O. Cohen, D. Hak, R. Nicolaescu, A. Fang, and M. Paniccia, Nature **433**, 294 (2005).
6. R. Claps, D. Dimitropoulos, V. Raghunathan, Y. Han, and B. Jalali, Opt. Express **11**, 1731 (2003).
7. R. L. Espinola, J. I. Dadap, R. M. Osgood, S. J. McNab, and Y. A. Vlasov, Opt. Express **12**, 3716 (2004).
8. J. I. Dadap, R. L. Espinola, R. M. Osgood, S. J. McNab, and Y. A. Vlasov, Opt. Lett. **29**, 2755 (2004).
9. Q. Xu, V. R. Almeida, and M. Lipson, Opt. Express **12**, 4437 (2004).
10. X. Chen, N. C. Panoiu, and R. M. Osgood, IEEE J. Quantum Electron. **42**, 160 (2006).
11. R. L. Espinola, J. I. Dadap, R. M. Osgood, S. J. McNab, and Y. A. Vlasov, Opt. Express **13**, 4341 (2005).
12. H. Rong, Y. Kuo, A. Liu, M. Paniccia, and O. Cohen, Opt. Express **14**, 1182 (2006).
13. M. A. Foster, A. C. Turner, J. E. Sharping, B. S. Schmidt, M. Lipson, and A. L. Gaeta, Nature **441**, 960 (2006).
14. O. Boyraz, P. Koonath, V. Raghunathan, and B. Jalali, Opt. Express **12**, 4094 (2004).
15. J. J. Wynne, Phys. Rev. **178**, 1295 (1969).
16. R. A. Soref and B. R. Bennett, IEEE J. Quantum Electron. **23**, 123 (1987).
17. G. P. Agrawal, Phys. Rev. Lett. **59**, 880 (1987).
18. J. A. Rothenberg, Phys. Rev. A **42**, 682 (1990).
19. G. P. Agrawal, *Nonlinear Fiber Optics* (Academic, 2001).
20. J. F. McMillan, X. Yang, N. C. Panoiu, R. M. Osgood, and C. W. Wong, Opt. Lett. **31**, 1235 (2006).